

The extinction of antimicrobial resistant pathogens using silver embedded silica nanoparticles and an efflux pump blocker

Jiya Jose¹, Abdulaziz Anas^{1*}, Bina Jose,¹ Anand Puthirath,² Sujith Athiyanathil,³ Chekidhenkuzhiyil Jasmin,¹ M. R. Anantharaman,² Shanta Nair,¹ Challapalli Subrahmanyam,⁴ Vasudevanpillai Biju^{5*}

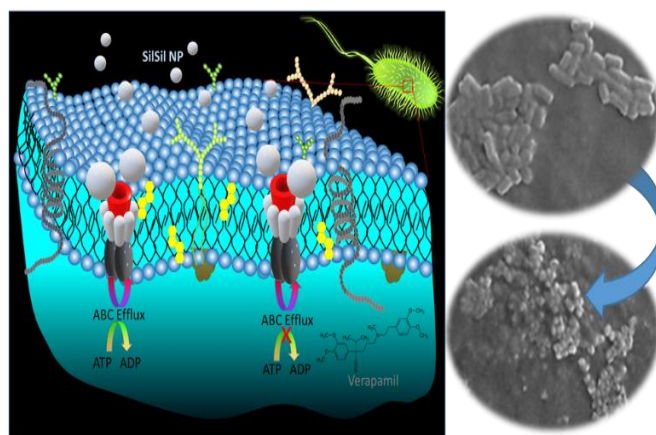
¹Council of Scientific and Industrial Research (CSIR)- National Institute of Oceanography (NIO), Regional Centre Cochin, Kerala, India, ²Cochin University of Science and Technology, Department of Physics, Cochin, Kerala, India, ³National Institute of Technology Calicut, Department of Chemistry, Calicut, Kerala, India, ⁴Department of Chemistry, Indian Institute of Technology Hyderabad, Kandi, Sangareddy, Teangana, India, ⁵Research Institute for Electronic Science, Hokkaido University, Sapporo 001-0020, Japan

Abstract

Control measures against antimicrobial resistant bacterial pathogens are important challenges in our daily life. In this study we discuss the sensitivity and resistance of four bacterial pathogens, *Vibrio alginolyticus*, *Escherichia coli*, *Staphylococcus aureus* and *Bacillus subtilis*, to silver-silica hybrid nanoparticles. Successively, by combining with an efflux pump blocking agent Verapamil, we find that these hybrid nanoparticles induce complete mortality to even the most resistive *S. aureus*. The above pathogens are selected from a pool of 100 bacterial strains resistant to silver nitrate. While *S. aureus* shows increased resistance to the nanoparticles, the cell wall integrity and genetic stability of *V. alginolyticus* and *E. coli* are compromised in the presence of the hybrid nanoparticles. These studies suggest that the antimicrobial properties of the nanoparticles against Gram negative pathogens originates from increased oxidative stress, which is confirmed by the blocking of reactive oxygen species (ROS) using scavengers such as ascorbic acid and observing DNA damage. The antimicrobial property of the nanoparticle when combined with its nontoxic nature to mammalian cells makes it a promising agent for controlling drug-resistant Gram-negative pathogens.

Key words: Pathogenic bacteria, silver-silica, hybrid nanoparticles, efflux pump, cytotoxicity, antimicrobial resistance

TOC Graphic



Antimicrobial resistance (AMR) is a global health threat, which impinges the effective prevention and treatment of bacterial infections.¹⁻⁴ The indiscriminate use of antibiotics in human, veterinary and aquaculture sectors have been considered to be the major cause of AMR.⁵⁻⁶ The emergence of resistance mechanisms by bacteria and the development of novel antibiotics have become a reciprocally evolving process which demands the continuous upgradation of the antimicrobial toolbox. Recently, nanomaterials and nanoscale platforms attract great attention to the detection⁷⁻⁹ and treatment¹⁰⁻¹⁴ of bacterial pathogens. Among such nanomaterials, silver-based nanoparticles are one of the most promising classes of antimicrobial agents for topical applications.^{13, 15} Although the antimicrobial properties of silver compounds are known for centuries, their medical use became insignificant with the discovery of antibiotics. With the emergence of bacterial resistance against mainstay antibiotics including carbapenems,¹⁶⁻¹⁷ silver-based treatment against AMR bacterial strains receives great attention. Also, the excellent localised surface plasmon resonance (LSPR) properties of silver nanoparticles (AgNPs) make them attractive to photothermal treatment against AMR bacterial strains. Indeed, the LSPR properties of AgNPs allow them to show excellent antimicrobial activities at lower concentrations when compared to the bulk silver such as in endotracheal tubes against pneumonia in photothermal treatment. It is hypothesized that AgNPs, on attachment to bacterial cell surface, can penetrate the cell membrane and release silver ion which inhibits the respiratory processes and the cell growth.¹⁸⁻²⁰ Previously, Ayala *et al.* reported the antibacterial properties of AgNPs against Methicillin resistant *Staphylococcus* strains.²¹ Apart from the antibacterial properties, AgNPs have been demonstrated to be promising antifungal²² and antiviral²³ agents.

Silver and its derivatives have been recorded historically as antimicrobial agents with minimum documented reports on emergence of resistance. Although the clinical application of silver compounds was displaced by antibiotics for a long time, co-evolution of antibiotic resistances among microorganisms re-introduced their importance. We envisage that the uncontrolled usage of AgNPs may lead to the same scenario of bacterial resistance soon because of metabolic versatility and inbuilt mechanisms of bacteria to overcome any adverse situations caused by metal ions. In the present study, we monitored the antibacterial properties of silver-silica nanoparticles (Sil-Sil NPs) against four environmental isolates of multiple metal and antibiotic resistant pathogens (*Vibrio alginolyticus*, *Escherichia coli*, *Staphylococcus aureus* and *Bacillus subtilis*), which were selected from a pool of 115 AgNO₃ resistant bacteria.

Sil-Sil NPs were prepared using a Sil-Sil sol and employing tetraethyl orthosilicate (TEOS), ethanol, distilled water and silver nitrate as precursors. The detailed procedure of nanoparticles synthesis and its characterization using X-ray powder diffractometer and transmission electron microscopy (TEM) technique are discussed elsewhere.²⁴ The particle size was analysed by dynamic light scattering technique in Zetasizer Nano Series (Malvern, UK) which can measure particle size in the range from 0.6 nm to 6 µm. The release of silver ions from Sil-Sil NP in phosphate buffered saline (PBS) was measured by inductively coupled plasma mass spectrometry (ICP-MS). Bacterial isolates (n=115) were obtained from a library of metal resistant bacteria, maintained at Marine Microbial Reference Facility (MMRF), Council of Scientific and Industrial Research (CSIR)-National Institute of Oceanography Regional Centre Cochin. The sensitivity of these isolates towards AgNO₃ was studied by monitoring their growth in a Luria Bertani medium containing different concentrations of metal ranging from 0.5 mM to 1000 mM. Antimicrobial effects of different concentrations of Sil-Sil NP on *Vibrio alginolyticus*, *Escherichia coli*, *Staphylococcus aureus* and *Bacillus subtilis* were studied following death rate assay.²⁵ The surface of *E. coli* and *S. aureus* were imaged before and after treatment with Sil-Sil NP, on a field emission scanning electron microscope (FESEM; Hitachi SU6600). The effect of Sil-Sil NPs on the cell wall integrity and DNA stability of test organisms in the presence and absence of an efflux pump blocker, Verapamil, were studied using SDS assay¹⁹ and comet assay²⁶ respectively. The role of efflux pump was also confirmed by PCR technique, amplifying the heavy metal efflux pump RND transporter gene using two sets of primer targeting chromosome (CusA F: 5'-TGGATGGGCTTTCATCTTTC and CusA R: 5'-TAACGCCTCATCCAGCTTCT) (NCBI accession No. U00096.2) plasmid (SilA F: 5'-GCAGAGTATCGAGGCGGTAG and SilA R: 5'-ACCTCCGATTGCTGAAGAGA) (NCBI accession No. AF067954) mediated resistance. The PCR products were cloned in pGEMT easy

vector, sequenced and the gene identity was confirmed by checking the sequence similarity in BLASTn in NCBI. The cytotoxicity of Sil-Sil NPs in mouse fibroblast cells (L929) were evaluated by 3-(4,5-dimethylthiazole-2-yl)-2,5-diphenyltetrazolium chloride (MTT) assay using MTT assay kit (Sigma Aldrich) according to the instructions by the manufacturer.

Almost all the isolates of bacteria were resistant to AgNO₃ at 1mM concentrations and a large majority, 60 – 65%, were resistant up to 1000 mM concentrations (Figure 1A). The sources of these isolates, their phylogeny, metal tolerance and ecological significance were discussed earlier.²⁷ Four representatives of pathogenic bacteria with high AgNO₃ resistant properties were further studied for their response towards Sil-Sil NPs. Interestingly, they showed differential responses toward Sil-Sil NPs (Figure 1B). Sil-Sil NPs highly toxic to Gram negative isolates and induced complete mortality at concentrations as low as 20 µg mL⁻¹. Among the Gram positive isolates, *B. subtilis* showed 80 % mortality rate at 20 µg mL⁻¹ concentration of Sil-Sil NPs. Surprisingly, *S. aureus* was highly-resistant to Sil-Sil NPs, recorded only 20 % mortality rate at 100 µg mL⁻¹ of Sil-Sil NPs.

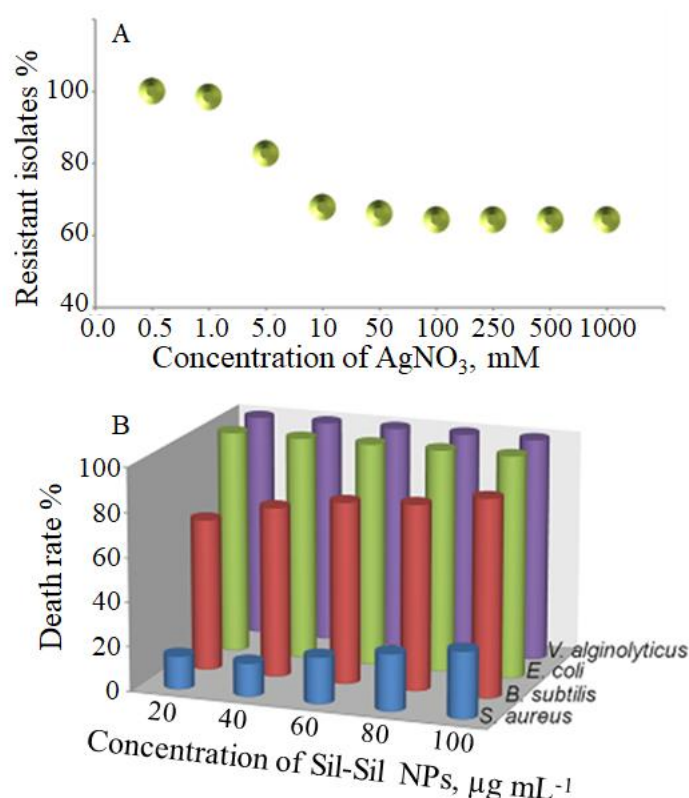


Figure 1: (A) Resistance pattern of bacterial isolates (115 Nos) against increasing concentrations of AgNO₃, (B) responses of AgNO₃ resistant bacterial isolates towards increasing concentrations of Sil-Sil NPs.

Silver nanoparticles are a more reactive form of silver, owing to their remarkable surface to volume ratios. ICP-MS analysis showed higher concentrations of silver dissolved from Sil-Sil NPs compared to that of AgNO₃ (Figure 2A). We observed less than 0.05 ppm of silver ions released from 500 mM

AgNO₃(i.e 8.5x10⁴μg mL⁻¹), whereas it was more than 0.2 ppm in 40 μgmL⁻¹ solution of Sil-Sil NPs. The silver ion release was retarded with increase in concentrations of Sil-Sil NPs. The particles used in the present study were monodispersed with an approximate size of 16 nm (Fig 2B). The available atoms on the surface of particle and the solubility and dissolution kinetics of silver ions increase with decreasing size of nanoparticles. For example, the surface atoms of 10 nm and 2 nm nanoparticles accounts for approximately 10 and 60 % of all atoms composing a crystalline particle. We observed approximately 4-fold higher concentration of dissolved silver in 20 μg mL⁻¹ solution of Sil-Sil NPs compared to 500 mM AgNO₃(i.e 85000 μg mL⁻¹). The solubility is related not only to the particle size but also the concentration of nanoparticles. Here, the dissolved silver concentration was reduced at 60, 80 and 100 μg mL⁻¹Sil-Sil NPs, which could be due to the aggregation of particles at higher concentration.

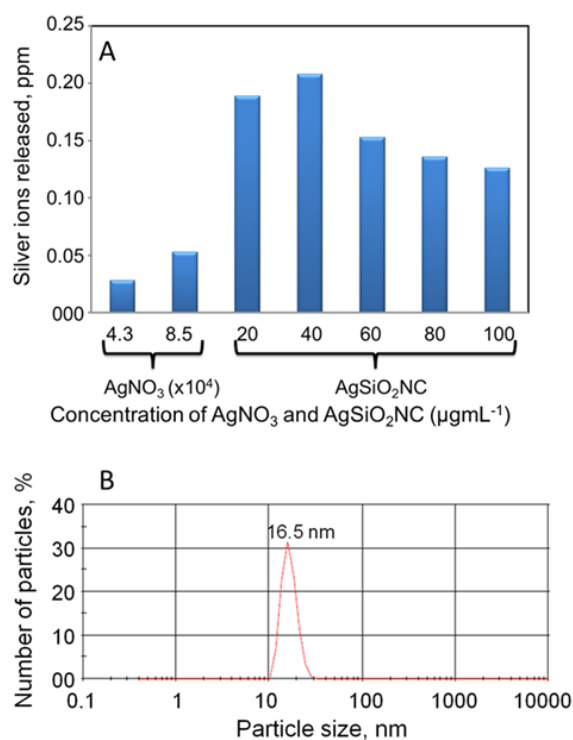


Figure 2: (A) Concentration of silver ions released from AgNO₃ and Sil-Sil NPs, and (B) the size distribution of Ag nanoparticles measured by dynamic light scattering technique.

Interestingly Sil-Sil NP at these concentrations was not toxic to mouse fibroblast cells, L929.

Figure 3A shows that more than 90 % of mouse fibroblast cells, L929, were viable in

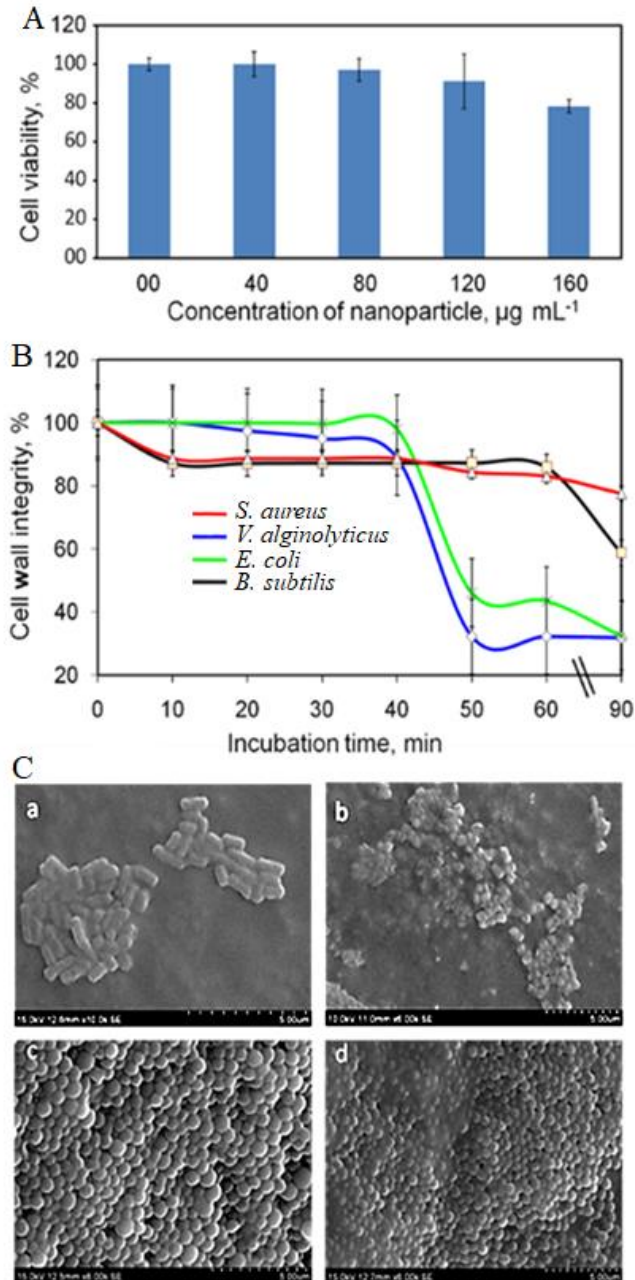


Figure 3: (A) Cytotoxicity of Sil-Sil NPs in mouse fibroblast cell, L929. Results are expressed as cell viability \pm standard deviation, (B) cell wall integrity of bacterial strains on exposure to Sil-Sil NPs for different time intervals. Results are expressed as cell wall integrity \pm standard deviation, and (C) Field emission scanning electron micrographs of *E. coli* (a, b) and *S. aureus* (c, d) before (a, c) and after (b, d) exposure to Sil-Sil NPs.

the presence of up to $120 \mu\text{g mL}^{-1}$ concentrations of Sil-Sil NPs. Approximately 80 % cells were viable at $160 \mu\text{g mL}^{-1}$ concentrations of Sil-Sil NPs. Unlike animal cells, bacteria are more sensitive to Sil-Sil NPs. These NPs severely impinge the cell wall integrity of Gram negative isolates, whereas Gram positive isolates were more resistant. Gram negative isolates recorded 70 % reduction in their cell wall integrity over a period of 90 min treatment with Sil-Sil NPs, while the Gram-positive isolate *B. subtilis* lost only 40 %. Interestingly, the cell wall of *S. aureus* was highly

resistant to Sil-Sil NPs, maintaining approximately 80 % integrity after 90 min exposure. The differential response of bacterial cell wall towards Sil-Sil NPs was further confirmed with scanning electron micrographs (Figure 3C). Cell surface of *E. coli* was severely damaged on exposure to Sil-Sil NPs, whereas there was no change for *S. aureus*. This difference may be attributed to the marked difference in the chemical and structural characteristics of Gram negative and positive bacterial cell walls.²⁸ Cell wall of a Gram negative *E. coli* is the first site of action of silver nanoparticles, where it instigates a chain of reactions including the expression of a number of envelop proteins (OmpA, OmpC, OmpF, OppA, and MetQ)¹⁹ and disruption of the barrier components.²⁹ Electron microscopy studies have revealed that majority of AgNPs are localized in the membranes of treated *E. coli* cells,³⁰ and that the particles at the size range of 10 nm can penetrate the cell membrane.³⁰⁻³¹ The extended layer of peptidoglycan on the cell wall of Gram-positive *S. aureus* may play pivotal role in preventing the cytoplasmic entry of nanoparticles protecting it from cell death. Inside the cytoplasm, silver nanoparticles interfere with respiratory chain reaction and³¹⁻³³nucleic acid stability,^{19, 34-35}and thus interfering with cell division leading to cell death.^{18, 36}

Since the genetic material of bacteria is not protected inside a nuclear membrane, they are freely accessible to internalized nanoparticles. Sil-Sil NP-induced DNA breakage is presented as a function of tail length in comet assay (Figure 4A). Representative images of comets formed are given in Figure 4B. Evidently, Sil-Sil NPs brought about a breakage in the DNA of Gram-negative isolates. However, the degree of breakage varied with the isolates; in this case 45 % of *E. coli* and 14 % *V. alginolyticus* incurred DNA breakage. The degree of DNA breakage was comparatively less in the case of Gram-positive isolates. Surprisingly 98 % of *S. aureus* cells were under low or no damage class in comet assays. Any breakage or damage to the genetic material of bacteria may lead to either mutation or death of organisms. Apart from forming stable adducts with purine and pyrimidine bases of nucleic acids, silver ions can replace native metal-cation prosthetic groups of DNA repair enzymes, leading to their inactivation^{18, 37} by intensifying oxidative damage of DNA. Inside the cytoplasm, silver ions initiate a cascade of reactions leading to the production of reactive oxygen species(ROS).¹⁵ ROS are a group of highly reactive species formed *via* the

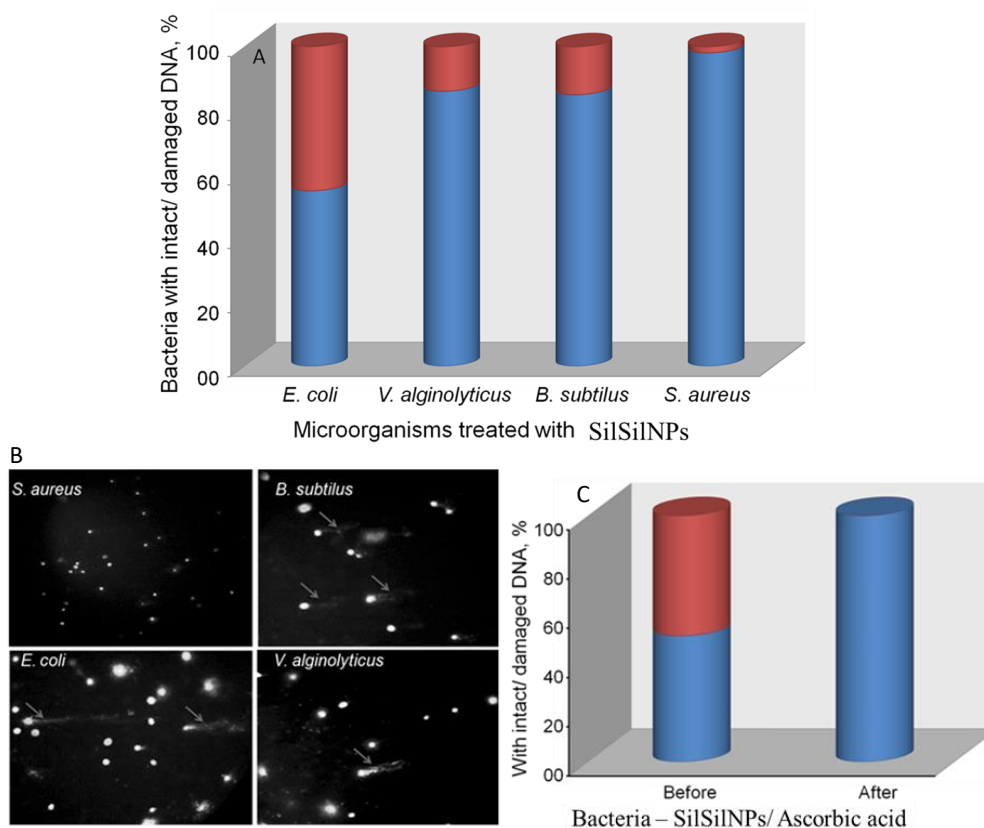


Figure 4: The effect of Sil-Sil NP on genetic stability of bacterial isolates; a. Comet assay histogram of bacterial isolates treated with Sil-Sil NPs ($100 \mu\text{g mL}^{-1}$) (Comets are classified based on tail length into intact (blue) and damaged (red)), b) representative images of comets (damaged DNA are marked) and c). Comet assay histogram of *E. coli* exposed to Sil-Sil NPs ($100 \mu\text{g mL}^{-1}$) in the presence (after) and absence (before) of ROS scavenger, ascorbic acid. The sizes of images in B are $0.2 \times 0.2 \text{ mm}^2$ (*S. aureus*) and $0.1 \times 0.1 \text{ mm}^2$ (other strains).

activation/reduction of molecular oxygen which includes singlet oxygen ($^1\text{O}_2$), superoxide anion ($\text{O}_2^{\bullet -}$), hydroxyl radical (HO^\bullet), and hydrogen peroxide (H_2O_2). Although minimum concentrations of ROS are necessary for maintaining the regular metabolism of cells, elevated levels can induce double strand breakages and nucleoside damages in DNA.³⁸ ROS creates a radical centre in the ribose group of DNA, which eventually cleaves the ribose phosphate bond, resulting in the breakage of DNA.³⁸ The role of ROS in Sil-Sil NP-induced DNA damage is confirmed by scavenging the ROS and free radicals using ascorbic acid. The DNA damage was completely absent in cells pre-incubated with the ROS scavenger, ascorbic acid, while 48 % cells showed DNA damage in groups treated only with Sil-Sil NPs.

Although antimicrobial properties of silver nanoparticles have been demonstrated against a wide range of Gram-positive and negative organisms, including multiple antibiotic resistant strains, the resistance against them are least discussed till date. The role of efflux pump in conferring resistance to *S. aureus* against Sil-Sil NPs was demonstrated by using Verapamil, an efflux pump inhibitor. Sil-

Sil NPs induce complete mortality of *S. aureus* when treated in the presence of Verapamil (Figure 5A), whereas those treated with Verapamil or Sil-Sil NP alone remained viable. In the presence of Verapamil, the Sil-Sil NPs could enter the cells and induce DNA damage among 57.5 % cells (Figure 5B). The role of the efflux pump was further confirmed by identifying the presence of

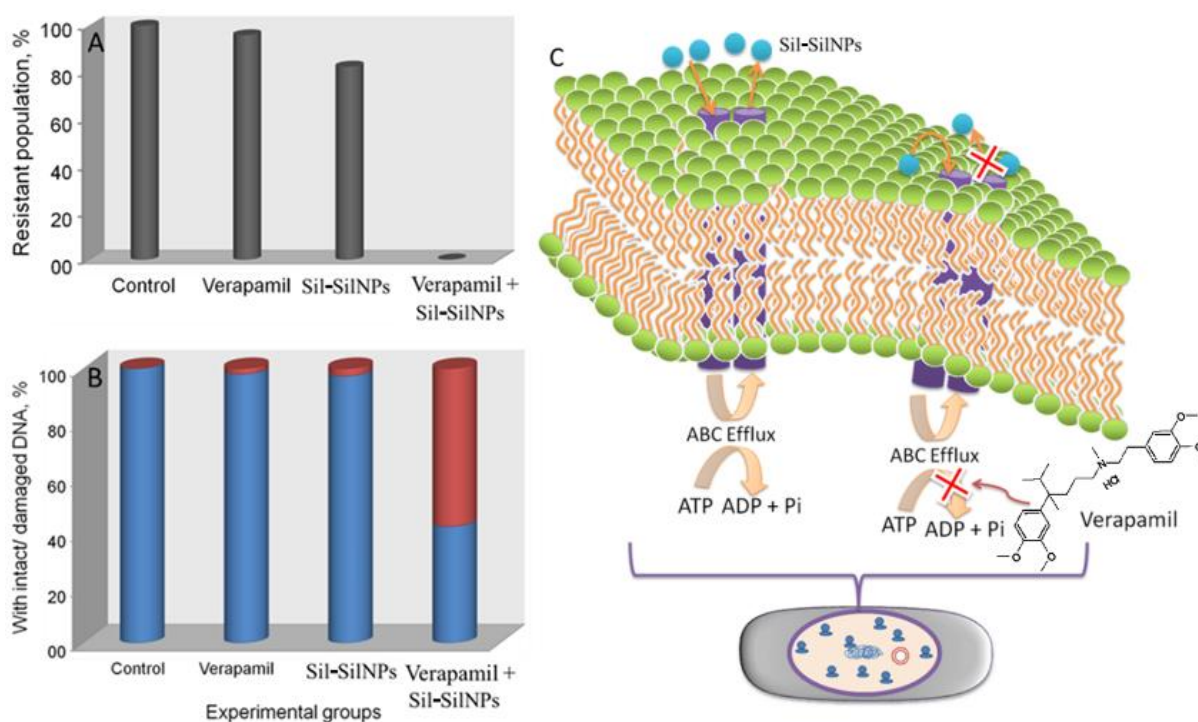


Figure 5: (A) Death rate and (B) comet assay histogram of *S. aureus* on exposure to Sil-Sil NPs in the presence and absence of the efflux pump inhibitor verapamil, and (C) schematic representation of the role of ABC efflux pump in conferring Sil-Sil NPs resistance to *S. aureus*.

genes responsible for heavy metal efflux transporter in the bacteria (Supplementary Figure1). The role and mechanisms of the efflux pump-mediated resistance towards silver ions are well discussed in the literature.³⁹ Based on these results, the mechanism of toxicity or resistance of bacteria against Sil-Sil NPs is schematically represented in Figure 5C.

We postulate that the efflux pump of *S. aureus* is versatile enough to protect it from the deleterious effects of Sil-Sil NPs which was confirmed by its blockade with Verapamil. Verapamil, a derivative of phenylalkylamine is an inhibitor of several bacterial ABC efflux pumps including LmrA and calcium channel antagonists.⁴⁰⁻⁴¹ Bacterial ABC transporters are assigned for the translocation of nutrients across the cell membrane and the same can be shared for conferring resistance towards toxic compounds.⁴¹ ABC efflux is an energy mediated process which includes a series of coordinated processes, starting with binding of the substrate with the transporter and hydrolysis of ATP, leading to critical rearrangements in the membrane spanning domains and uni-dimensional substrate translocation.⁴¹ Once the toxicants are expelled from the cytoplasm,

transporters inactivate themselves through the dissociation of ADP and inorganic phosphorous. Based on recording the death rate after blocking the ATP hydrolysis step of ABC efflux using Verapamil, it is apparent that the ABC transporter proteins play a key role in conferring Sil-Sil NP resistance to *S. aureus*.

In short, the present study underlines the enhanced antibacterial properties of silver-silica nanoparticles against AgNO₃ and antimicrobial resistant pathogenic bacteria such as *V.alginolyticus* and *E. coli*. The nanoparticles disintegrate the cell wall of Gram-negative bacteria and induce DNA damage by upregulating the oxidative stress. On the other hand, experiments with Gram-positive bacterial strains suggest that their efflux pumps can protect them from accumulation and antibacterial actions of silver-silica nanoparticles. Furthermore, the nanoparticles are nontoxic to mammalian cells. Results in the current study suggest that the silver-based nanoparticles are also amenable to bacterial resistance, and hence sufficient precautions may be taken in their wide spread application.

ASSOCIATED CONTENT

Supporting Information. The following Supporting Information is available free of charge on the ACS Publications website at DOI: xxxxx.

Agarose gel image of heavy metal efflux pump RND transporter gene, and experimental details of preparation of Sil-Sil NPs, sensitivity of bacterial isolates towards AgNO₃ and Sil-Sil NPs, SEM imaging, cytotoxicity assay, the effect of Sil-Sil NP on cell wall integrity (SDS assay), the effect of Sil-Sil NP on stability of DNA (comet assay), efflux pump of *S. aureus* and antibacterial property of Sil-Sil NPs.

AUTHOR INFORMATION

Corresponding Authors

*E-mail: biju@es.hokudai.ac.jp.

*E-mail: anas@nio.org.

ORCID

Vasudevanpillai Biju: 0000-0003-3650-9637

Author contributions

AA, MMRIA, CS, VB and SN are involved in the design of experiment, data analysis and writing of manuscript. JJ and BJ are involved in the microbiology related experiments, ABP was responsible

for the synthesis of nanoparticles, ABP along with SA contributed to structural characterization of nanoparticles. AA and JC are contributed to molecular analysis and toxicity in animal cell lines. AA, CS and VB prepared the manuscript.

Notes

The authors declare no competing financial interest.

ACKNOWLEDGEMENTS

The authors thank the Director, CSIR-National Institute of Oceanography, Goa, and the Scientist-in-charge, NIO, RC-Kochi for extending all necessary support. JJ is thankful for the fellowships given by CSIR-SRF programme. VB acknowledges financial support from MEXT under the JSPS grant-in-aid for scientific research B (19H02550) and the JSPS Core-to-Core Program. CS and VB acknowledge support (SPARC) from the Science and Engineering Board (SERB) of India and the Japan International Cooperation Agency (JICA).

REFERENCES AND NOTES

- (1) Ingle, D. J.; Levine, M. M.; Kotloff, K. L.; Holt, K. E.; Robins-Browne, R. M. Dynamics of antimicrobial resistance in intestinal *Escherichia coli* from children in community settings in South Asia and sub-Saharan Africa. *Nature Microbiology* **2018**,*3*, 1063 – 1073
- (2) Barlow, G. Clinical challenges in antimicrobial resistance. *Nature Microbiology* **2018**,*3*, 258 – 260.
- (3) Woolhouse, M.; Farrar, J. An intergovernmental panel on antimicrobial resistance. *Nature* **2014**,*509*, 555 – 557.
- (4) Sugden, R.; Kelly, R.; Davies, S. Combatting antimicrobial resistance globally. *Nature Microbiology* **2016**,*1*, 16187.
- (5) Walsh, T. R. A one-health approach to antimicrobial resistance. *Nature Microbiology* **2018**,*3*, 854 – 855.
- (6) Jorgensen, P. S.; Wernli, D.; Carroll, S. P.; Dunn, R. R.; Harbarth, S.; Levin, S. A.; So, A. D.; Schluter, M.; Laxminarayan, R. Use antimicrobials wisely. *Nature* **2016**,*537*, 159 – 161.
- (7) Syal, K.; Iriya, R.; Yang, Y.; Yu, H.; Wang, S.; Haydel, S. E.; Chen, H.-Y.; Tao, N. Antimicrobial Susceptibility Test with Plasmonic Imaging and Tracking of Single Bacterial Motions on Nanometer Scale. *ACS Nano* **2016**,*10* (1), 845-852, DOI: 10.1021/acsnano.5b05944.
- (8) Li, X.; Kong, H.; Mout, R.; Saha, K.; Moyano, D. F.; Robinson, S. M.; Rana, S.; Zhang, X.; Riley, M. A.; Rotello, V. M. Rapid Identification of Bacterial Biofilms and Biofilm Wound Models Using a Multichannel Nanosensor. *ACS Nano* **2014**,*8* (12), 12014-12019, DOI: 10.1021/nm505753s.
- (9) Mezger, A.; Fock, J.; Antunes, P.; Østerberg, F. W.; Boisen, A.; Nilsson, M.; Hansen, M. F.; Ahlford, A.; Donolato, M. Scalable DNA-Based Magnetic Nanoparticle Agglutination Assay for Bacterial Detection in Patient Samples. *ACS Nano* **2015**,*9* (7), 7374-7382, DOI: 10.1021/acsnano.5b02379.
- (10) Xiao, F.; Cao, B.; Wang, C.; Guo, X.; Li, M.; Xing, D.; Hu, X. Pathogen-Specific Polymeric Antimicrobials with Significant Membrane Disruption and Enhanced Photodynamic Damage

- To Inhibit Highly Opportunistic Bacteria. *ACS Nano* **2019**,*13* (2), 1511-1525, DOI: 10.1021/acsnano.8b07251.
- (11) Some, S.; Ho, S.-M.; Dua, P.; Hwang, E.; Shin, Y. H.; Yoo, H.; Kang, J.-S.; Lee, D.-k.; Lee, H. Dual Functions of Highly Potent Graphene Derivative–Poly-L-Lysine Composites To Inhibit Bacteria and Support Human Cells. *ACS Nano* **2012**,*6* (8), 7151-7161, DOI: 10.1021/nn302215y.
 - (12) Xi, Y.; Ge, J.; Guo, Y.; Lei, B.; Ma, P. X. Biomimetic Elastomeric Polypeptide-Based Nanofibrous Matrix for Overcoming Multidrug-Resistant Bacteria and Enhancing Full-Thickness Wound Healing/Skin Regeneration. *ACS Nano* **2018**,*12* (11), 10772-10784, DOI: 10.1021/acsnano.8b01152.
 - (13) Kim, T.; Zhang, Q.; Li, J.; Zhang, L.; Jokerst, J. V. A Gold/Silver Hybrid Nanoparticle for Treatment and Photoacoustic Imaging of Bacterial Infection. *ACS Nano* **2018**,*12* (6), 5615-5625, DOI: 10.1021/acsnano.8b01362.
 - (14) Pang, X.; Xiao, Q.; Cheng, Y.; Ren, E.; Lian, L.; Zhang, Y.; Gao, H.; Wang, X.; Leung, W.; Chen, X.; Liu, G.; Xu, C. Bacteria-Responsive Nanoliposomes as Smart Sonotheranostics for Multidrug Resistant Bacterial Infections. *ACS Nano* **2019**,*13* (2), 2427-2438, DOI: 10.1021/acsnano.8b09336.
 - (15) AshaRani, P., Mun, G.L.K., Hande, M.P., Valiyaveetil, S. Cytotoxicity and genotoxicity of silver nanoparticles in human cells. *ACS Nano* **2009**,*3*, 279-290.
 - (16) Walsh, T. R.; Weeks, J.; Livermore, D. M.; Toleman, M. A. Dissemination of NDM-1 positive bacteria in the New Delhi environment and its implications for human health: an environmental point prevalence study. *Lancet Infectious Diseases* **2011**,*11*, 355 - 362.
 - (17) Yong, G.; Toleman, M. A.; Giske, C. G.; Cho, H. S.; Sundman, K.; Lee, K.; Walsh, T. R. Characterization of a new metallo- β -lactamase gene, *bla*NDM-1, and a novel erythromycin esterase gene carried on a unique genetic structure in *Klebsiella pneumoniae* sequence type 14 from India. *Antimicrobial Agents and Chemotherapy* **2009**,*53* (12), 5046 - 5054.
 - (18) Li, W.-R.; Xie, X.-B.; Shi, Q.-S.; Zeng, H.-Y.; OU-Yang, Y.-S.; Chen, Y.-B. Antibacterial activity mechanism of silver nanoparticles on *Escherichia coli*. *Applied Microbiology and Biotechnology* **2010**,*85*, 1115 - 1122.
 - (19) Lok, C. N.; Ho, C. M.; Chen, R.; He, Q. Y.; Yu, W. Y.; Sun, H.; Tam, P.-H.; Chiu, J.-F.; Che, M. Proteomic analysis of the mode of antibacterial action of silver nanoparticles. *Journal of Proteome Research* **2006**, *5* (916 - 924).
 - (20) Morones, J. R.; Elechiguerra, J. L.; Camacho-Bragado, A.; Holt, K.; Kouri, J. B.; Tapina, J. The bactericidal effect of silver nanoparticles. *Nanotechnology* **2005**,*2005* (16).
 - (21) Ayala-Nunez, N. V.; Villegas, H. H. L.; Turrent, L. d. C. I.; Padilla, C. R. Silver nanoparticles toxicity and bactericidal effect against methicillin resistant *Staphylococcus aureus*: Nanoscale does matter. *Nanobiotechnology* **2009**,*5*, 2 - 9.
 - (22) Ogar, A.; Tylko, G.; Turnau, K. Antifungal properties of silver nanoparticles against indoor mould growth. *Science of The Total Environment* **2015**,*521-522*, 305-314, DOI: <https://doi.org/10.1016/j.scitotenv.2015.03.101>.
 - (23) Elechiguerra, J. L.; Burt, J. L.; Morones, J. R.; Camacho-Bragado, A.; Gao, X.; Lara, H. H. Interaction of silver nanoparticles with HIV-1. *Journal of Nanobiotechnology* **2005**,*3*, 6.
 - (24) Thomas, S.; Nair, S. K.; Muhammad Abdul Jamal, A.; Al-Harhi, S. H.; Varma, M. R.; Anantharaman, M. R. Size-dependent surface plasmon resonance in silver silica nanocomposites. *Nanotechnology* **2008**,*19*, 075710 (7pp).
 - (25) Asok, A.; Arshad, E.; Jasmin, C.; Somnath Pai, S.; Bright Singh, I. S.; Mohandas, A.; Anas, A. Reducing *Vibrio* load in *Artemia nauplii* using antimicrobial photodynamic therapy: a promising strategy to reduce antibiotic application in shrimp larviculture. *Microbial Biotechnology* **2012**,*5* (1), 59-68.

- (26) Singh, N. P.; Stephens, R. E.; Singh, H.; Lai, H. Visual quantification of DNA double strand breaks in bacteria. *Mutation Research* **1999**,*429*, 159 - 168.
- (27) Jose, J.; Giridhar, R.; Anas, A.; Loka Bharathi, P. A.; Nair, S. Heavy metal pollution exerts reduction/adaptation in the diversity and enzyme expression profile of heterotrophic bacteria in Cochin estuary, India. *Environmental Pollution* **2011**,*159*, 2775 - 2780.
- (28) Beveridge, T. J. Role of cellular design in bacterial metal accumulation and mineralization. *Annual Review of Microbiology* **1989**,*43*, 147 - 171.
- (29) Vara, M. Agents that increase the permeability of the outer membrane *Microbiology Reviews* **1992**,*56*, 395 - 411.
- (30) Sondi, I., Salopek-Sondi. Silver nanoparticles as antimicrobial agent: a case study on E. coli as a model for Gram-negative bacteria. . *Journal of Colloid Interface Science*. **2004**,*275*, 177 - 182.
- (31) Xu, X. H.; Brownlow, W. I.; Kyriacou, S. V.; Wan, Q.; Viola, J. J. Real-time probing of membrane transport in living microbial cells using single nanoparticle optics and living cell imaging. *Biochemistry* **2004**,*43*, 10400 - 10413.
- (32) Dibrov, P.; Dzioba, J.; Gosink, K. K.; Hase, C. C. Chemiosmotic mechanism of antimicrobial activity of Ag⁺ in *Vibrio cholerae*. *Antimicrobial Agents and Chemotherapy* **2002**,*46*, 2668 - 2670.
- (33) Schreuers, W. I., Rosenberg, H., . Effect of silver ions on transport and retention of phosphate by *Escherichia coli*. . *Journal of Bacteriology* **1982**,*152*, 7 - 13.
- (34) Feng, Q. I.; Wu, J. L.; Chen, G., Q; Cui, F. Z.; Kim, T. N.; Kim, J. O. A mechanistic study of the antibacterial effect of silver ions on *Escherichia coli* and *Staphylococcus aureus*. *Journal of Biomedical Material Research* **2000**,*52*, 662 - 668.
- (35) Ghandour, W., Hubbard, J.A., Deistung, J., Hughes, M.N., Poole, R.K.,. The uptake of silver ions by *Escherichia coli* K 12: Toxic effects and interaction with copper ions. *Applied Microbiology and Biotechnology* **1994**,*28*, 559 - 565.
- (36) Rai, M.; Yadav, A.; Gade, A. Silver nanoparticles as a new generation of antimicrobials. *Biotechnology Advances* **2009**,*27*, 76 - 83.
- (37) Wang, Y.; Li, J.; Wang, H.; Jin, J.; Liu, J.; Wang, K.; Tan, W.; Yang, R. Silver ions- mediated conformational switch: Facile design of structure - controllable nucleic acid probes. *Analytical Chemistry* **2010**,*82*, 6607 - 6612.
- (38) Anas, A.; Akita, H.; Harashima, H.; Itoh, T.; Ishikawa, M.; Biju, V. Photosensitized breakage and Damage of DNA by CdSe-ZnS quantum dots. *Journal of Physical Chemistry B* **2008**,*112*, 10005 - 10011.
- (39) Chacón, K. N.; Mealman, T. D.; McEvoy, M. M.; Blackburn, N. J. Tracking metal ions through a Cu/Ag efflux pump assigns the functional roles of the periplasmic proteins. *Proceedings of the National Academy of Sciences of the United States of America* **2014**,*111* (43), 15373-15378, DOI: 10.1073/pnas.1411475111.
- (40) Zechini, B.; Versace, I. Inhibitors of multidrug resistant efflux systems in bacteria. *Recent Patents on Anti-Infective Drug Discovery* **2009**,*4*, 37 - 50.
- (41) Locher, K. P.; Lee, A. T.; Rees, D. C. The *E. coli* BtuCD structure: A framework for ABC transporter architecture and mechanism. *Science* **2002**,*296*, 1091 - 1098.

The extinction of antimicrobial resistant pathogens using silver embedded silica nanoparticles and an efflux pump blocker

Jiya Jose,¹ Abdulaziz Anas,^{1,*} Bina Jose,¹ Anand Puthirath,² Sujith Athiyanathil,³ Chekidhenkuzhiyil Jasmin,¹ M. R. Anantharaman,² Shanta Nair,¹ Challapalli Subrahmanyam,⁴ Vasudevanpillai Biju^{5,*}

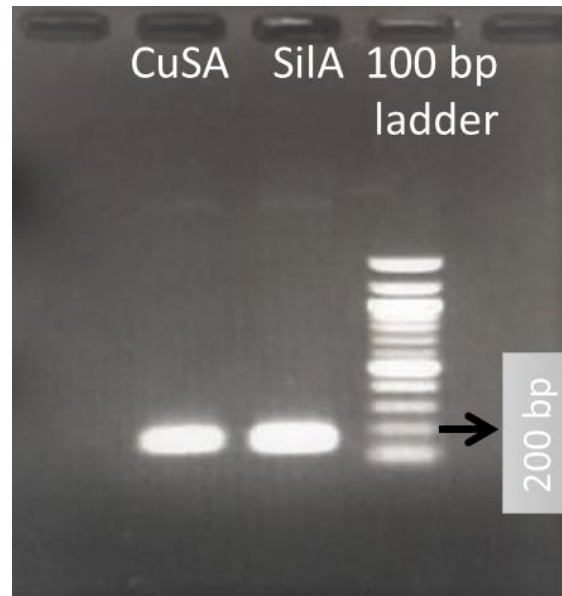


Figure S1: Agarose gel image of heavy metal efflux pump RND transporter gene amplified using two sets of primer targeting chromosome (CusA) and plasmid (SilA) mediated genes

EXPERIMENTAL SECTION

Silver–silica nanoparticles (Sil-Sil NPs)

Sil-Sil NP was prepared using Sil-Silsol and employing tetraethyl orthosilicate (TEOS), ethanol, distilled water and silver nitrate as precursors. The detailed procedure of nanoparticles synthesis and its characterization using X-ray powder diffractometer and transmission electron microscopy (TEM) technique are discussed elsewhere.²⁴ The particle size was analysed by dynamic light scattering technique in Zetasizer Nano Series (Malvern, UK) which can measure particle size in the range from 0.6 nm to 6 μ m. The release of silver ions from Sil-Sil NP in phosphate buffered saline (PBS) was measured by inductively coupled plasma mass spectrometry (ICP-MS).

Bacterial Culture

Bacterial isolates (n=115) were obtained from a library of metal resistant bacteria, maintained at Marine Microbial Reference Facility (MMRF), Council of Scientific and Industrial Research (CSIR)-National Institute of Oceanography Regional Centre Cochin. Bacterial isolates were inoculated into

Luria Bertani (LB) broth and was grown overnight at $28 \pm 2^\circ\text{C}$ in an orbital shaker at 120 rpm and subcultured weekly. The purity of the cultures was confirmed by staining and fatty acid profiles.

Sensitivity of bacterial isolates towards AgNO₃ and Sil-Sil NPs

One hundred and fifteen bacterial isolates were tested for AgNO₃ resistance by spot inoculating on LB agar containing different concentrations of AgNO₃ ranging from 0.5 mM to 1000 mM. The cultures showing growth in AgNO₃ enriched media in 48 h was considered as resistant strain.

Antimicrobial effects of different concentrations of Sil-Sil NP on *Vibrio alginolyticus*, *Escherichia coli*, *Staphylococcus aureus* and *Bacillus subtilis* are expressed as % death rate. Briefly, micro-centrifuge tubes containing 10^6 cells mL⁻¹ were exposed separately to 0, 20, 40, 60, 80 and 100 µg mL⁻¹ concentrations of Sil-Sil NP for 1 h, and bacterial growth enumerated on LB agar plates. All plates were incubated at $28 \pm 2^\circ\text{C}$ for 24 h to enumerate the total number of colonies. Death rate was calculated using the equation:

$$\text{Death rate \% } (\epsilon) = \frac{(N_1 - N_2) \times 100}{N_1}$$

Scanning Electron Microscopy

The surface of *E. coli* and *S. aureus* were imaged before and after treatment with Sil-Sil NP, which on a field emission scanning electron microscope (FESEM; Hitachi SU6600). The samples were prepared by placing washed and dehydrated cells on a microscope sample holder and gold sputtering in an argon atmosphere. Adequate care was exercised to obtain homogenous cell gold coating.

Cytotoxicity assay

Cytotoxicity of Sil-Sil NP was evaluated by 3-(4,5-dimethylthiazole-2-yl)-2,5-diphenyltetrazolium chloride (MTT) assay following standard protocol. Here, $\sim 10^6$ mouse fibroblast cells (L929) were inoculated into 96-well tissue culture plate containing DMEM supplemented with 10% FBS and incubated for 24 h at 37 °C. The cells were washed three times with PBS, and the medium was exchanged with DMEM containing different concentrations of Sil-Sil NP (0, 40, 80, 120 and 160 µg mL⁻¹) in triplicate. The cells were incubated for 12 h at 37 °C and assayed using MTT assay kit (Sigma Aldrich) according to the instructions by the manufacturer.

The effect of Sil-Sil NP on cell wall integrity – SDS assay

The effect of Sil-Sil NP on cell wall integrity of test organisms were investigated by SDS assay following the method of Lok et al.¹⁹ Briefly, overnight cultures of bacterial cells were washed

copiously with sterile phosphate buffered saline and dispensed in the wells of a sterile microplate to a volume of 200 μL . After measuring the initial absorbance, the test solution was supplemented with Sil-Sil NP ($100 \mu\text{g mL}^{-1}$) and SDS (0.1 %). Control wells without Sil-Sil NP were maintained. The absorbance at 600 nm was recorded at every 15 min for a period of 2 h. The percent decrease in absorbance compared to the initial reading was plotted against time.

The effect of Sil-Sil NP on stability of DNA- Comet assay

The effect of Sil-Sil NP on the stability of genetic material was investigated by comet assay following the method of Singh et al.²⁶ Briefly, 10^6 bacterial cells were mixed with 500 μL of 0.5 % low melting point agarose prepared in TAE buffer containing RNase ($5 \mu\text{g mL}^{-1}$), SDS (10 %) and lysozyme (0.5 mg mL^{-1}), and spread over a microscopic slide pre-coated with a thin layer of 0.5 % agarose. Subsequently, the cell wall of bacteria was digested by incubating in a lysis solution (containing NaCl (0.15 M), Tris (pH 10, 10 mM), EDTA (100 mM) and Triton X100 (1 %) followed by proteinase K treatment for 2 h at 37 °C. The slides were equilibrated with 300 mM sodium acetate and electrophoresed at 50 V for 15-20 min. Following electrophoresis, the slides were immersed in 1 M ammonium acetate in ethanol for 30 min, and then in absolute ethanol for 1 h, air dried at 25 °C, immersed in 70 % ethanol for 30 min and dried. Slides were stained with 1 ml freshly prepared solution of 1 μl SyBr green in TE buffer. The comets were recorded using a fluorescent microscope (Olympus BX 51) equipped with filter pairs (470-490 nm: Excitation filter, 520 nm: Emission filter, 500 nm: Dichroic filter) and CCD camera. The comet length was measured and processed using the software Image Pro. The comets were classified based on tail length as intact (0-10 μm length), and damaged (>10 μm) groups, and expressed as % number of incidence in the histogram. The role of reactive oxygen species (ROS) on Sil-Sil NP induced DNA damaged was assayed by adding ascorbic acid, ROS scavenger, to reaction mixture before adding Sil-Sil NPs.

$$\text{Number of incidence, \%} = \frac{\text{Number of cells in each class}}{\text{Total cells counted}} \times 100$$

Efflux pump of *S. aureus* and antibacterial property of Sil-Sil NPs

The role of efflux pump in conferring resistance to *S. aureus* to Sil-Sil NP was investigated using comet assay. Briefly *S. aureus* were exposed to Verapamil, calcium channel blocker for ABC transporter, to a final concentration of $20 \mu\text{g mL}^{-1}$ for 1 h prior to the treatment with Sil-Sil NP. Death rate and nucleic acid damage of cells were determined following the method explained above. The role of efflux pump was confirmed by PCR technique, amplifying the heavy metal efflux pump RND transporter gene using two sets of primer targeting chromosome (CusA F: 5'-

TGGATGGGCTTTCATCTTTC and CusA R: 5'- TAACGCCTCATCCAGCTTCT) (NCBI accession No. U00096.2) plasmid (SilA F: 5'- GCAGAGTATCGAGGCGGTAG and SilA R:5'- ACCTCCGATTGCTGAAGAGA) (NCBI accession No. AF067954) mediated resistance. The PCR conditions followed was; initial denaturation (95 °C for 2 min), followed by cycle denaturation (at 94 °C for 30 s), annealing (at 60 °C for 30 s), extension (at 72 °C for 30 s) for a total of 30 cycles and a final extension for 5 min at 72 °C. In the PCR, 5 µl DNA sample was used as template for 50 µl reaction mixture containing 2 µl each of primers (10 picomoles µl⁻¹), 5 µl 10X Taq polymerase buffer (NEB, Canada), 1 U Taq DNA polymerase (NEB, Canada) and 200 µM dNTPs (NEB, Canada). The PCR products were cloned in pGEMT easy vector, sequenced and the gene identity was confirmed by checking the sequence similarity in BLASTn in NCBI.